Research Square

Preprints are preliminary reports that have not undergone peer review.
They should not be considered conclusive, used to inform clinical practice,
or referenced by the media as validated information.

Morphological, Histochemical, and Proteomic Analysis of the Effects of Fluoride and Amoxicillin, with Calcium and Vitamin D Supplementation, on Dental Enamel Formation.

Isabel Maria Porto

isabel.porto@unesp.br

UNESP https://orcid.org/0009-0004-5496-2114

André Acácio Souza da Silva

UNIFESP

Julia Alves dos Santos

UNESP

Betânia Mansor Silva

UNESP

Enzo Bacelar Giacomin

UNESP

Gabrielle Sampaio da Fonseca

UNESP

Raquel Fernanda Gerlach

USP

Research Article

Keywords: Enamel, fluoride, amoxicillin

Posted Date: January 8th, 2026

DOI: https://doi.org/10.21203/rs.3.rs-8532261/v1

License: This work is licensed under a Creative Commons Attribution 4.0 International License.
Read Full License

Additional Declarations: The authors declare no competing interests.

Abstract

Ameloblasts are the cells exclusively responsible for enamel formation. Although this process is genetically regulated, external factors such as fluoride and amoxicillin can interfere with enamel development. Some studies suggest that calcium supplementation may reduce the deleterious effects of fluoride on enamel. The aim of this study was to evaluate whether fluoride and/or amoxicillin impair ameloblast viability and enamel formation, and whether calcium and vitamin D supplementation reduce the potential damage caused by these substances to dental enamel. Although calcium and vitamin D administration increased the superficial resistance of enamel to acid challenge, hydroxyapatite crystals were disorganized in the inner enamel of the experimental groups. Ameloblasts exhibited apoptotic bodies and positive staining for caspase-3 and TUNEL. KLK4 levels were reduced within ameloblasts from fluoride-treated groups but the abundance increased in the enamel matrix. In addition, the abundance of AMBN, AMTN, and ODAM in the matrix was reduced. No statistical differences in abundance of amelogenins was observed. These findings indicate that fluoride exposure, exacerbated by concomitant amoxicillin use, compromises multiple axes of amelogenesis, resulting in a structurally disorganized and functionally weakened enamel.

Introduction

Dental enamel is the most highly mineralized tissue in the body, comprising approximately 95% mineral content at the end of its mineralization process [1]. For complete enamel maturation to occur, the organic matrix must be almost entirely removed from the enamel matrix [2, 3]. During the mineralization stage, the protease responsible for cleaving enamel proteins is kallikrein-4 (KLK4), a serine protease secreted by ameloblasts [4–5]. Although amelogenesis is genetically regulated [6], it can be affected by external factors such as fluoride and amoxicillin [7, 8].

Fluoride, despite its well-known beneficial effects on enamel [9, 10], can cause structural damage when present in excess, leading to dental fluorosis [10]. The threshold between acceptable and toxic fluoride levels is very narrow. Amoxicillin has also been associated with enamel defects, such as white spot lesions, and with the development of molar–incisor hypomineralization (MIH) [11–13].

Ameloblasts are the epithelial cells exclusively responsible for amelogenesis. Damage to these cells can severely affect enamel quality, since ameloblasts are lost after tooth eruption and enamel does not undergo remodeling [14]. Consequently, damage occurring during enamel formation cannot be repaired. Several studies have reported that fluoride induces cellular stress in ameloblasts, leading to cellular dysfunction and potentially cell death [15–17]. Caspase-3 is a key enzyme in the apoptotic pathway [18]. Some studies suggest that calcium supplementation reduces the severity of fluorosis [19, 20], and vitamin D administration enhances calcium absorption [21].

Thus, the aim of this study was to investigate whether fluoride and/or amoxicillin impair ameloblast viability and enamel formation by analyzing ameloblast and enamel matrix morphology, KLK4 production by ameloblasts, evidence of ameloblast cell death, and the proteomic profile of enamel matrix proteins

involved in hydroxyapatite crystal organization. In addition, we evaluated whether calcium and vitamin D supplementation reduce the potential damage caused by fluoride and/or amoxicillin to dental enamel.

Methods

Animals and Experimental Design

The experimental protocol was approved by the Ethics Committee of the School of Dentistry of Araraquara (process no. 01/2023). A total of 80 male Holtzman rats (*Rattus norvegicus albinus*), aged 2–3 months and weighing 190–210 g, were used in this study.

Animals were treated for 60 days with fluoride, amoxicillin, and calcium plus vitamin D, administered either individually or in combination. Rats were randomly assigned to eight experimental groups (n = 10 per group):

(I) control, (II) fluoride, (III) fluoride + amoxicillin, (IV) amoxicillin, (V) fluoride + vitamin D + calcium, (VI) amoxicillin + vitamin D + calcium, (VII) vitamin D + calcium, and (VIII) fluoride + amoxicillin + vitamin D + calcium.

At the end of the treatment period, animals were euthanized. Urine samples were collected for fluoride quantification; hemimandibles were harvested for morphological analyses (light microscopy, transmission and scanning electron microscopy, and immunohistochemistry); and upper and lower incisors were collected for calcium and phosphate quantification and proteomic analysis.

Description of Experimental Groups

Control: animals received water and food *ad libitum* for 60 days.

Fluoride: animals received 45 mg fluoride/L (100 mg sodium fluoride/L) in drinking water for 60 days, with food provided *ad libitum*.

Vitamin D + Calcium (VitD + Ca): animals received 2.0 g calcium carbonate/150 g chow and 7000 IU/week vitamin D, administered intragastrically, for 60 days. Water and food were provided *ad libitum*.

Amoxicillin (Amx): animals received amoxicillin (500 mg/kg body weight) as an oral suspension, administered intragastrically every 24 h for 60 days, following Souza et al. (2021). Water and food were provided *ad libitum*.

Fluoride + Amoxicillin (F + Amx): animals received 45 mg fluoride/L in drinking water and amoxicillin (500 mg/kg body weight) administered intragastrically every 24 h for 60 days.

Fluoride + Vitamin D + Calcium (F + VitD + Ca): animals received 45 mg fluoride/L in drinking water, 2.0 g calcium carbonate/150 g chow, and 7000 IU/week vitamin D for 60 days, with food and water *ad libitum*.

Amoxicillin + Vitamin D + Calcium (Amx + VitD + Ca): animals received amoxicillin (500 mg/kg/day), 2.0 g calcium carbonate/150 g chow, and 7000 IU/week vitamin D for 60 days. Water and food were provided *ad libitum*.

Fluoride + Amoxicillin + Vitamin D + Calcium (F + Amx + VitD + Ca): animals received fluoride, amoxicillin, calcium, and vitamin D according to the protocols described above, with water and food provided *ad libitum* for 60 days.

Throughout the experimental period, daily food and water intake per animal were recorded, and body weight was monitored every 15 days.

Urinary Fluoride Quantification

Urinary fluoride concentration was determined to assess fluoride excretion. On the day of euthanasia, urine was directly aspirated from the bladder using a 1-mL syringe fitted with a fine-gauge needle. Samples were stored at − 20°C until analysis.

Prior to measurement, urine samples were mixed with TISAB II (pH 5.0) at a 1:1 ratio. Fluoride concentration was determined using a fluoride-selective ion electrode (Orion Star A214 Analyzer) calibrated with standard solutions ranging from 0.125 to 32 µg F/mL. Results are expressed as mg F/L. Differences between groups were analyzed by One-way ANOVA. The significance level was set as 0.05 ($p < 0.05$).

Macroscopic analysis of the lower incisors

The labial surface of the lower incisors was photographed to record alterations caused by fluoride and amoxicillin in the brownish coloration of the teeth.

Phosphorus Quantification for Estimation of Enamel Mass Loss by Acid Biopsy

Phosphorus quantification was used to estimate the amount of enamel (mg) removed by acid biopsy. Five rat incisors per group were analyzed according to the method described by [22]. Briefly, the labial surface of the incisal third of the lower incisors was immersed for 20 s in 500 µL of 1.8% nitric acid.

Phosphorus concentration was determined using the Fiske and Subbarow colorimetric method, as described by [23]. Measurements were performed in triplicate at 660 nm using a spectrophotometer (DR 2500, Hach, Loveland, USA). Calibration curves were generated using phosphorus standards at 1, 2, 4, and 8 mg/mL. Enamel mass loss was calculated assuming that enamel contains 17.4% phosphorus [24]. Differences between groups were analyzed by One-way ANOVA. The significance level was set as 0.05 ($p < 0.05$).

Scanning Electron Microscopy (SEM)

Five lower incisors per group were ground under water cooling to a thickness of 500 µm, as measured with a digital caliper. Specimens were etched with 37% phosphoric acid gel for 30 s, sonicated for 10 min, fixed in 4% paraformaldehyde, dehydrated through a graded acetone series, mounted on aluminum stubs, carbon-coated, and examined by scanning electron microscopy.

Light Microscopy

Light microscopy was used to evaluate enamel matrix structure and ameloblast morphology. Five hemimandibles per group were dissected and fixed in 4% buffered paraformaldehyde (pH 7.2) for 48 h. Specimens were decalcified in 7% EDTA (pH 7.2), dehydrated through graded ethanol, cleared in xylene, and embedded in paraffin. Sections (5 µm) were obtained and stained with hematoxylin and eosin (H&E).

TUNEL Assay

Deparaffinized sections mounted on silanized slides were processed using the ApopTag Peroxidase In Situ Apoptosis Detection Kit (Merck, USA), according to the manufacturer's instructions. Sections were pretreated with proteinase K (20 µg/mL; Sigma-Aldrich) for 15 min at room temperature, followed by incubation with 3% hydrogen peroxide to quench endogenous peroxidase activity. Terminal deoxynucleotidyl transferase (TdT) labeling was performed at 37°C for 1 h. The reaction was stopped, and sections were incubated with anti-digoxigenin–peroxidase for 30 min. Immunoreactivity was visualized using 3,3'-diaminobenzidine (DAB; Sigma-Aldrich), followed by counterstaining with Carazzi's hematoxylin.

Immunohistochemistry

The kallikrein-4 and cleaved caspase-3 imunohistochemestry is described as following. Deparaffinized sections were subjected to antigen retrieval in sodium citrate buffer (pH 6.0) using a pressure cooker at 90°C for 30 min. Endogenous peroxidase activity was quenched with 3% hydrogen peroxide. Sections were then incubated overnight at 4°C with anti-cleaved caspase-3 (Cell Signaling Technology, USA) or anti-kallikrein-4 (Abcam, ab231048, USA) diluted 1:200. Immunodetection was performed using the Vectastain Elite ABC Universal Plus Kit (Vector Laboratories), with ImmPACT DAB used as the chromogen. Sections were counterstained with Carazzi's hematoxylin. For each slide containing two serial sections, one section served as a positive control, while the other served as a negative control in which the primary antibody was omitted and replaced with PBS.

KLK4 Immunolabeled area quantification

The measurement of the KLK 4 immunolabelled areas was performed in images acquired with a Leica DFC 550 camera attached to a Leica BM4000 B LED microscope, and a Leica Application Suite (LAS 4.3)

software. The KLK 4 immunolabelled area was measured across two non-consecutive sections per animal. The analysis was performed in a standardized total ameloblast epithelial areas (post secretory ameloblast region), and the immunopositively area per μm² of epithelium was calculated for KLK 4 marker. To ensure consistency, parameters for threshold, color range, hue, and saturation were kept constant for the marker.

Ameloblast layer height

due to the difficulty in identifying the end of the secretory stage and the onset of enamel mineralization, the height of ameloblasts in the region where KLK4 quantification was performed, was measured to ensure that, across groups, the ameloblasts were at the same stage of amelogenesis (post-secretory stage). The ameloblast layer height was measured in two non-consecutive sections per animal, in each section 3 pictures of the post secretory ameloblast region were taken and the epithelial height in μm was measured three times in each picture, totaling 30 measurements per animal.

Statistical analysis

Statistical analyses were performed using GraphPad Prism 10.2.3 software (GraphPad Software, CA, USA). To examine whether the samples were normally distributed, the normality test (Shapiro–Wilk test) was applied. Differences between groups were analyzed by One-way ANOVA. The significance level was set as 0.05 ($p < 0.05$).

Liquid Chromatography Mass Spectrometry (LC–MS/MS) Analysis

Five upper incisors per group were used for protein extraction. The labial enamel surface was immersed for 5 min in 500 μL of 10% HCl containing protease inhibitors (N-ethylmaleimide, phenanthroline, and phenylmethylsulfonyl fluoride; 2 mM each). Protein extracts were desalted using ZipTip C18 tips (Merck Millipore) and eluted with 50% acetonitrile/0.1% trifluoroacetic acid (TFA).

Peptides were analyzed by LC–MS/MS using an Orbitrap Exploris 240 mass spectrometer (Thermo Fisher Scientific, USA) coupled to an Evosep One liquid chromatography system via a nanoelectrospray ion source, operated in data-independent acquisition (DIA) mode. Peptides were loaded onto EV2001 C18 Evotips and separated on an IonOpticks Aurora Elite™ XT C18 UHPLC column (15 cm × 75 μm, 1.7 μm particle size) using the Evosep Whisper Zoom 20SPD method (20 samples/day).

The nanoelectrospray voltage was set to 1.7 kV, and the ion source temperature was maintained at 275°C. Full MS scans were acquired at a resolution of 120,000 over an m/z range of 350–1400, with an automatic gain control (AGC) target of 300% and a maximum injection time of 45 ms. MS/MS spectra were acquired using 34 DIA windows, each spanning 20 m/z units (361–1033 m/z), at a resolution of 15,000, with an AGC target of 1000% and a normalized collision energy of 27%.

Proteomic Data Processing:

Data-independent acquisition (DIA) raw files were processed using Spectronaut v19 (Biognosys, Zurich, Switzerland) with the directDIA workflow and default settings, against the Rattus norvegicus UniProt database (22,403 entries; downloaded September 2025). Peptide identification was performed using an unspecific enzyme, allowing peptide lengths of 7–52 amino acids, up to two missed cleavages, and up to five variable modifications. Methionine oxidation and protein N-terminal acetylation were specified as variable modifications. Identification thresholds were set to precursor Q-value < 0.01, precursor posterior error probability (PEP) < 0.2, protein (experiment) Q-value < 0.01, protein (run) Q-value < 0.05, and protein PEP < 0.75. Protein-level quantitative values (PG.Log2Quantity) were exported from the Experiment Analysis report (PG_Quantity sheet) at the protein group (PG.ProteinGroups) aggregation level. Only protein groups with non-missing quantitative values were retained for downstream analyses. Exported intensities were already $\log_2$-transformed, and no additional global transformation was applied. MS2-based quantities (PG.MS2Quantity) were not used for the primary differential abundance analysis. For each experiment, runs were classified according to the Run label defined in Spectronaut and used to generate three independent pairwise comparisons: fluoride vs. control, amoxicillin vs. control, and fluoride + amoxicillin vs. control. For each contrast, PG.Log2Quantity values corresponding to control and treated samples were extracted from the PG_Quantity sheet and grouped by experimental condition.

Per-Protein Summarization and Differential Abundance Analysis

All statistical analyses were performed in R (version 2025.09.2). For each pairwise comparison, a working dataset (pg_stats) was generated from the PG_Quantity sheet and included protein group identifiers (PG.ProteinGroups), gene symbols (PG.Genes), $\log_2$-transformed quantitative values for individual runs (PG.Log2Quantity), and derived summary statistics. For each protein group and comparison, the mean $\log_2$ intensity was calculated separately for control and treated samples as the mean across all runs within each condition (rowMeans, na.rm = TRUE). The $\log_2$ fold change ($\log_2$FC) was defined as:

$$log FC = mean_{treated} - mean_{control},$$

with positive values indicating higher protein abundance in the treated group and negative values indicating higher abundance in controls.

Differential abundance was assessed using a two-sided unpaired Student's t-test applied to $\log_2$ intensities for each protein group. Resulting p values were calculated using the base R t.test function. Proteins with insufficient variability or entirely missing values across conditions were assigned NA and excluded from statistical inference. Correction for multiple testing within each comparison was performed using the Benjamini–Hochberg procedure, yielding the false discovery rate (FDR). The primary criterion for differential abundance was FDR < 0.05. Given the modest sample size and the limited number of proteins meeting this stringent threshold, additional exploratory criteria were applied, as described below.

Volcano and Venny Plot Visualization:

For data visualization and hypothesis generation, volcano plots were constructed for each pairwise comparison using ggplot2. For each protein group, $\log_2$ fold change ($\log_2$FC) was plotted on the x-axis, and either $-\log_{10}$(FDR) or $-\log_{10}$(p value) was plotted on the y-axis, as appropriate. Vertical dashed lines were drawn at $|\log_2 FC| = 0.58$, corresponding to an approximate 1.5-fold change, and horizontal dashed lines were placed at FDR = 0.05 or nominal p = 0.05.

Because none or only a limited number of proteins met the stringent FDR < 0.05 criterion, exploratory candidate sets were defined using more permissive thresholds. First, proteins with $|\log_2 FC| > 0.58$ ($\approx \geq$ 1.5-fold change), irrespective of FDR, were used to describe overall patterns of protein up- and downregulation across treatments. Second, proteins with $|\log_2 FC| > 0.58$ and nominal $p < 0.05$ (unadjusted) were highlighted in volcano plots (red, increased abundance in treated groups; blue, decreased abundance) and exported; their corresponding FDR values were reported but not used as strict cutoffs.

To visualize treatment-associated changes in key proteins, heatmaps were generated based on $\log_2$ fold-change ($\log_2$FC) values derived from the differential proteomic analysis (treated vs. control). For each comparison (fluoride vs. control, amoxicillin vs. control, and fluoride + amoxicillin vs. control), protein-level $\log_2$FC values were calculated from the $\log_2$-transformed Spectronaut intensities as described above, also a venny diagram [25] was constructed with the proteins with downregulated abundance and the proteins related with enamel formation was highlighted.

The union of all selected genes across the three comparisons was used to construct a gene × contrast matrix (rows = proteins; columns = fluoride, amoxicillin, fluoride + amoxicillin).

All R scripts used for data processing and visualization are available from the corresponding author upon reasonable request.

Results

Average Daily Water and Food Intake

The addition of sodium fluoride to drinking water and calcium carbonate to the diet did not impair palatability, as daily water and food intake were comparable to or, in some groups, higher than those of controls (data not shown). Based on fluoride concentration in drinking water and average daily intake, estimated fluoride ingestion was approximately 100-fold higher in fluoride-treated groups (2.10–2.42 mg/animal/day) compared with non-fluoride–treated groups (0.02–0.03 mg/animal/day).

Urinary Fluoride

Urinary fluoride concentration in rats treated with fluoride was markedly higher, as expected (mean 8.33 mgF/L ± 3.99 in fluoride-treated groups versus 0.76 mgF/L ± 0.35 in the other groups). This indicates

that, in animals receiving sodium fluoride salts added to the drinking water, the amount of circulating fluoride in the organism was substantially higher—on the order of tenfold—compared with groups in which fluoride was not added to the water. The table with data of fluoride concetration in urine is shown in Table 1 of Supplemental Data.

Brownish pigmentation caused by the treatment

The lower incisors of the fluoride-treated groups exhibited defects in the brownish pigmentation, showing a pattern of alternating light and dark striations. The width of these striations was increased in the teeth of animals treated with fluoride + amoxicillin. The remaining groups (including those treated with amoxicillin alone) did not show any alterations (Fig. 1).

Vitamin D and calcium improved surface enamel and not enamel organization

Phosphorus-based quantification of acid biopsy samples revealed group-dependent differences in enamel acid resistance. Enamel from the fluoride + vitamin D + calcium and amoxicillin + vitamin D + calcium groups exhibited greater resistance to acid challenge, with approximately 14 mg of enamel removed, whereas the fluoride-only group showed the highest susceptibility, with approximately 31 mg of enamel removed (Fig. 2).

Scanning electron microscopy revealed disorganization of hydroxyapatite prisms in groups treated with fluoride and/or amoxicillin, either individually or in combination. The prismatic enamel in the groups treated with fluoride and/or amoxicillin appeared thinner, resulting in a wider interprismatic enamel band and exhibiting focal voids within the enamel matrix. These ultrastructural alterations persisted in animals receiving calcium and vitamin D supplementation, suggesting that although supplementation may improve surface enamel characteristics, it does not prevent deeper prism disorganization associated with fluoride and amoxicillin exposure (Fig. 3).

Fluoride and Amoxicillin causes ameloblasts death

H&E-stained sections revealed apoptotic bodies in ameloblasts and within the enamel organ epithelium, particularly near the proximal region, in the amoxicillin, fluoride + amoxicillin, and fluoride + amoxicillin + vitamin D + calcium groups. These alterations were most evident during the transition between the late secretory and early maturation stages (Figs. 4a-c).

TUNEL staining confirmed the presence of apoptotic cells, with DAB-positive nuclei and bodies identified both within ameloblasts and in the adjacent enamel organ epithelium (Figs. 4e-f). The apoptotic process was more pronounced in the group that received concomitant administration of fluoride and amoxicillin (Fig. 4f).

Immunohistochemical analysis for caspase-3 revealed positive staining for caspase-3 in some ameloblasts from the fluoride, amoxicillin and fluoride + amoxicillin, (Fig. 5). The positive reaction to caspase-3 was more pronounced in the groups that received fluoride (Figs. 5c-d). Calcium and vitamin D supplementation did not modify the differences observed among the experimental groups, nor did it promote significant changes when compared to the control group.

Fluoride treatment causes disturbances in KLK4

Quantification of KLK4 in the ameloblast layer showed a statistically lower amount of this protease within ameloblasts, indicating that fluoride interferes with the production of this protein by ameloblasts. Measurements of the ameloblast layer in which KLK4 quantification was performed showed no differences among groups, confirming that the analyses were carried out at the same stage of amelogenesis (post-secretory stage) (Fig. 6). Calcium and vitamin D supplementation did not modify the differences observed among the experimental groups, nor did it promote significant changes when compared to the control group.

Fluoride and Amoxicillin treatment alters enamel proteins abundance

Overall, the amoxicillin group exhibited the highest number of downregulated proteins. Focusing on proteins closely related to ameloblast metabolic activity or enamel matrix mineralization, both the amoxicillin and fluoride + amoxicillin groups showed the strongest downregulation profiles. Ameloblastin (AMBN) was consistently downregulated across all experimental groups compared to controls (Fig. 7a).

Comparative proteomic analysis between the fluoride-treated and control groups demonstrated that the enamel matrix of fluorotic animals exhibited increased abundance of KLK4, accompanied by reduced abundance of odontogenic ameloblast-associated protein (ODAM) and AMBN (fold change ≤ 1.5; $p < 0.05$) (Fig. 7b).

In the comparison between the amoxicillin-treated and control groups, the experimental group showed decreased abundance of AMBN (fold change ≤ 1.5; $p < 0.05$) (Fig. 7a).

Similarly, comparison of the fluoride + amoxicillin and control groups revealed downregulation of amelotin (AMTN) and AMBN, along with upregulation of KLK4 in the experimental group (fold change ≤ 1.5; $p < 0.05$) (Fig. 7c).

The heatmap comparing the three experimental groups with the control group revealed a greater inhibition of AMBN expression in the groups treated with amoxicillin. In contrast, ODAM showed reduced expression in the fluoride-treated groups. AMTN was downregulated exclusively in the fluoride plus amoxicillin (F + Amx) group. In addition, KLK4 quantity was increased in all three experimental groups, with a more pronounced upregulation in the fluoride-treated groups (Fig. 6d). Calcium and vitamin D

supplementation did not modify the differences observed among the experimental groups, nor did it promote significant changes when compared to the control group.

Discussion

Proper dental enamel mineralization depends on the almost complete removal of the organic matrix and water, allowing mineral influx and growth in the thickness and width of hydroxyapatite crystals, a process that is strictly dependent on the functional integrity of ameloblasts [26]. In this study, exposure to fluoride and/or amoxicillin did not alter the palatability of water or feed, but it promoted profound structural changes in enamel. Although calcium and vitamin D supplementation increased superficial acid resistance of the enamel, scanning SEM revealed prism disorganization in the deeper layers, indicating that supplementation was not sufficient to prevent treatment-induced structural damage, contrary to previous studies reporting that calcium supplementation reduces fluoride-induced damage [27, 28]. Other studies found no differences in crystals between fluorotic and control groups [29, 30], whoever, Bronckers et al. [31] reported that fluoride interferes with crystal shape and size at ultrastructural levels.

In parallel, histological analysis and cell death detection assays demonstrated a significant increase in apoptotic bodies and TUNEL-positive and caspase-3 labeling in ameloblasts, particularly during the transition from the secretory to the maturation stage. This effect was more pronounced when fluoride and amoxicillin were administered concomitantly, suggesting a negative synergistic effect on the viability and homeostasis of these cells, which are essential for amelogenesis. Consistent with our findings, Sahlberg et al. [32] reported detachment of ameloblasts from the enamel matrix, along with alterations in enamel secretion and mineralization, in an in vitro model after exposure to amoxicillin alone or in combination with fluoride. Souza et al. [33] did not observe increased fluoride damage when amoxicillin was administered concomitantly, nor enamel alterations with amoxicillin alone. Kumazawa et al. [34] found no ameloblast alterations after a single amoxicillin injection.However, other studies have associated amoxicillin use with enamel formation defects, such as altered molar and incisor mineralization [11].

These cellular alterations are directly reflected in the proteomic profile of the enamel matrix. Immunohistochemistry revealed reduced KLK4 in ameloblasts from fluoride-treated groups, whereas mass spectrometry analysis demonstrated increased KLK4 retained in the enamel matrix, indicating that fluoride not only compromises its production by ameloblasts but also its removal from the matrix, a process that is fundamental for enamel protein degradation during maturation. Den Besten et al. [35] reported the influence of fluoride on the amount of active proteinases during the enamel maturation stage. Sharma et al. [15] associated decreased KLK4 transcription with ameloblast cellular stress induced by fluoride. In contrast, Tye et al. [36] concluded that fluoride does not directly alter KLK4 secretion. Suzuki et al. [37] related reduced KLK4 mRNA transcription to decreased TGF-β1 expression induced by fluoride, given evidence of KLK4 regulation by TGF-β1, whereas Li et al. [16] attributed decreased KLK4 expression to reduced Forkhead box O1 (Foxo1) expression induced by sodium fluoride.

The consistente abundance reduction of AMBN in treated groups is particularly relevant, as this protein has been proposed to act as a nucleator in hydroxyapatite crystal formation in enamel [38, 39], serving as a scaffold for initial crystal formation and growth [40]. Decreased AMBN suggests early impairment of cell–matrix interactions, rendering enamel more susceptible to the structural disorganization observed.

In the fluoride + amoxicillin group, a reduction in AMTN was also observed. This protein is expressed during the mineralization stage and plays a critical role in enamel formation, indicating that there is an additional potential impairment in the final processes of enamel hardening and surface quality [41]. Like AMTN, ODAM acts as a nucleator of hydroxyapatite crystals in the enamel matrix. Its abundance was reduced in the fluoride and fluoride + amoxicillin groups, which may explain the crystal disorganization observed by SEM.

Some studies suggest that fluoride increases secretory activity and protein production by secretory ameloblasts, and that post-secretory ameloblasts are unable to remove all this organic content, thereby increasing protein retention in the enamel matrix [42]. Denbesten et al. [43] described the effect of fluoride in reducing smooth-ended ameloblasts, which are responsible for efficient removal of the organic enamel matrix. Fluorotic enamel, despite having a hypermineralized surface, exhibits a subsurface region with protein retention [44, 45]. Our findings suggest that fluoride decreases KLK4 production by ameloblasts, a protease responsible for cleavage of enamel proteins during the maturation stage, as well as reducing the secretion of enamel proteins such as AMBN, AMTN, and ODAM, which are essential for proper hydroxyapatite crystal formation. In addition, fluoride leads to inefficient removal of certain proteins, such as KLK4, which remain retained in the enamel matrix.

In conclusion, our findings indicate that fluoride exposure, exacerbated by concomitant amoxicillin use, compromises multiple axes of amelogenesis—ameloblast viability, matrix proteolysis, protein secretion, and mineral maturation—resulting in a structurally disorganized and functionally weakened enamel.

Declarations

Authors

Porto IM[1*], da Silva AAS[2], dos Santos JVA[1], Silva BM[1], Giacomin EB[1], da Fonseca GS[1], Gerlach RF[3].

Conflict of Interest

The authors declare that there is no conflict of interest.

Acknowledgements:

We thank Professor Cinthia Pereira Machado Tabchoury from the Department of Biosciences, Piracicaba Dental School (UNICAMP), for fluoride determination in the samples; the Department of Cell and Molecular Biology and Pathogenic Bioagents of the Ribeirão Preto Medical School (USP) for the SEM images; and the Brazilian National Laboratory of Biosciences (LNBio/CNPEM) for the mass spectrometry analysis. We are deeply grateful for the financial support provided by the State São Paulo Research Foundation (FAPESP), research grant no. 2023/08752-3.

References

1. Robinson C, Kirkham J, Brookes SJ, Bonass A, Shore RC (1995) The chemistry of enamel development. Int J Dev Biol 39:145–152
2. Reith EJ (1970) The stages of amelogenesis as observed in molar teeth of young rats. J Ultrastruct Res 30:111–151. https://doi.org/10.1016/s0022-5320(70)90068-7
3. Kallenbach E (1971) Electron microscopy of the differentiating rat incisor ameloblast. J Ultrastruct Res 35:508–531. https://doi.org/10.1016/s0022-5320(71)80008-4
4. Hu CC, Ryu OH, Chen JJ, Uchida T, Wakida K, Murakami C, Jiang H, Qian Q, Zhang C, Ottmers V, Bartlett JD, Simmer JP (2009) Cloning of the murine EMSP1 cDNA and analysis of expression during tooth development. J Dent Res 79:70–76. https://doi.org/10.1177/00220345000790011301
5. Simmer JP, Fukae M, Tanabe T, Yamakoshi Y, Uchida T, Zhu J, Margolis HC, Hu CC, Bartlett JD (1998) Purification, characterization and cloning of enamel matrix serine proteinase 1. J Dent Res 77:377–386. https://doi.org/10.1177/00220345980770020601
6. Lu Y, Papagerakis P, Yamakoshi Y, Hu JC, Bartlett JD, Simmer JP (2008) Functions of KLK4 and MMP-20 in dental enamel formation. Biol Chem 389:695–700. https://doi.org/10.1515/BC.2008.080
7. Evans RW, Stamm JW (1991) Dental fluorosis following downward adjustment of fluoride in drinking water. J Public Health Dent 51:91–98. https://doi.org/10.1111/j.1752-7325.1991.tb02187.x
8. Beentjes VE, Weerheijm KL, Groen HJ (2002) Factors involved in the aetiology of molar–incisor hypomineralisation (MIH). Eur J Paediatr Dent 3:9–13
9. Aoba T (1997) The effect of fluoride on apatite structure and growth. Crit Rev Oral Biol Med 8:136–153. https://doi.org/10.1177/10454411970080020301
10. Aoba T, Fejerskov O (2002) Dental fluorosis: chemistry and biology. Crit Rev Oral Biol Med 13:155–170. https://doi.org/10.1177/154411130201300206
11. Laisi S, Ess A, Sahlberg C, Arvio P, Lukinmaa PL, Alaluusua S (2009) Amoxicillin may cause molar incisor hypomineralization. J Dent Res 88:132–136. https://doi.org/10.1177/0022034508328334
12. Wuollet E, Laisi S, Salmela E, Ess A, Alaluusua S (2016) Molar-incisor hypomineralization and the association with childhood illnesses and antibiotics in a group of Finnish children. Acta Odontol Scand 74:416–422. https://doi.org/10.3109/00016357.2016.1172342
13. Souza JF, Costa-Silva CM, Jeremias F, Santos-Pinto L, Zuanon AC, Cordeiro RC (2012) Molar incisor hypomineralisation: possible aetiological factors in children from urban and rural areas. Eur Arch

Paediatr Dent 13:164–170. https://doi.org/10.1007/BF03262865

14. Laisi S, Kiviranta H, Lukinmaa PL, Vartiainen T, Alaluusua S (2008) Molar-incisor-hypomineralisation and dioxins: new findings. Eur Arch Paediatr Dent 9(4):224–227. https://doi.org/10.1007/BF03262639
15. Sharma R, Tsuchiya M, Skobe Z, Tannous BA, Bartlett JD (2010) The acid test of fluoride: how pH modulates toxicity. PLoS ONE 5:e10895. https://doi.org/10.1371/journal.pone.0010895
16. Li W, Jiang B, Cao X, Xie Y, Huang T (2017) Protective effect of lycopene on fluoride-induced ameloblast apoptosis and dental fluorosis through oxidative stress-mediated caspase pathways. Chem Biol Interact 261:27–34. https://doi.org/10.1016/j.cbi.2016.11.021
17. Suzuki M, Bandoski C, Bartlett JD (2015) Fluoride induces oxidative damage and SIRT1/autophagy through ROS-mediated JNK signaling. Free Radic Biol Med 89:369–378. https://doi.org/10.1016/j.freeradbiomed.2015.08.015
18. Kari S, Subramanian K, Altomonte IA, Murugesan A, Yli-Harja O, Kandhavelu M (2022) Programmed cell death detection methods: a systematic review and a categorical comparison. Apoptosis 27:482–508. https://doi.org/10.1007/s10495-022-01735-y
19. Patel PP, Patel PA, Zulf MM, Yagnik B, Kajale N, Mandlik R et al (2017) Association of dental and skeletal fluorosis with calcium intake and serum vitamin D concentration in adolescents from a region endemic for fluorosis. Indian J Endocrinol Metab 21:190–195. https://doi.org/10.4103/2230-8210.196013
20. Bhowmik AD, Shaw P, Mondal P, Chakraborty A, Sudarshan M, Chattopadhyay A (2021) Calcium and vitamin D supplementation effectively alleviates dental and skeletal fluorosis and retain elemental homeostasis in mice. Biol Trace Elem Res 199:3035–3044. https://doi.org/10.1007/s12011-020-02435-x
21. Foster BL, Nociti FH Jr, Somerman MJ (2014) The rachitic tooth. Endocr Rev 35(1):1–34. https://doi.org/10.1210/er.2013-1009
22. Sawan RMM, Leite GAS, Saraiva MCP, Barbosa F Jr, Tanus-Santos JE, Gerlach RF (2010) Fluoride increases lead concentrations in whole blood and in calcified tissues from lead-exposed rats. Toxicology 271:21–26. https://doi.org/10.1016/j.tox.2010.02.002
23. Costa de Almeida GR, Saraiva MCP, Barbosa F Jr, Kurg FJ, Cury JA, Sousa ML, Buzalaf MAR, Gerlach RF (2007) Lead contents in the surface enamel of deciduous teeth sampled in vivo from children in uncontaminated and lead-contaminated areas. Environ Res 104:337–345. https://doi.org/10.1016/j.envres.2007.03.007
24. Halse A, Selvig KA (1974) Mineral content of developing rat incisor enamel. Eur J Oral Sci 82:40–46. https://doi.org/10.1111/j.1600-0722.1974.tb01899.x
25. Oliveros JC (2007–2015) Venny. An interactive tool for comparing lists with Venn's diagrams. https://bioinfogp.cnb.csic.es/tools/venny/index.html
26. Porto IM, Merzel J, de Sousa FB, Bachmann L, Cury JA, Line SR, Gerlach RF (2009) Enamel mineralization in the absence of maturation stage ameloblasts. Arch Oral Biol 54(4):313–321.

https://doi.org/10.1016/j.archoralbio.2009.01.007

27. Lyaruu DM, Blijleven N, Hoeben-Schornagel K, Bronckers AL, Wöltgens JH (1989) X-ray micro-analysis of the mineralization patterns in developing enamel in hamster tooth germs exposed to fluoride in vitro during the secretory phase of amelogenesis. Adv Dent Res 3(2):211–218. https://doi.org/10.1177/08959374890030022201
28. Bronckers AL, Bervoets TJ, Wöltgens JH, Lyaruu DM (2006) Effect of calcium, given before or after a fluoride insult, on hamster secretory amelogenesis in vitro. Eur J Oral Sci 114(Suppl 1):116–122. https://doi.org/10.1111/j.1600-0722.2006.00307.x
29. Fejerskov O, Johnson NW, Silverstone LM (1974) The ultrastructure of fluorosed human dental enamel. Scand J Dent Res 82:357–372. https://doi.org/10.1111/j.1600-0722.1974.tb00389.x
30. Robinson C, Yamamoto K, Connell SD, Kirkham J, Nakagaki H, Smith AD (2006) The effects of fluoride on the nanostructure and surface pK of enamel crystals. Eur J Oral Sci 114(Suppl 1):99–104. https://doi.org/10.1111/j.1600-0722.2006.00275.x
31. Bronckers AL, Lyaruu DM, DenBesten PK (2009) The impact of fluoride on ameloblasts and the mechanisms of enamel fluorosis. J Dent Res 88:877–893. https://doi.org/10.1177/0022034509343280
32. Sahlberg C, Pavlic A, Ess A, Lukinmaa PL, Salmela E, Alaluusua S (2013) Combined effect of amoxicillin and sodium fluoride on the structure of developing mouse enamel in vitro. Arch Oral Biol 58:1155–1164. https://doi.org/10.1016/j.archoralbio.2013.03.007
33. Souza JF, Costa SA, Busanelli DG, Santos-Pinto L, Cerri PS, Cury JA, Tenuta L, Cordeiro RC (2021) In vivo effect of fluoride combined with amoxicillin on enamel development in rats. J Appl Oral Sci 29:e20210171. https://doi.org/10.1590/1678-7757-2021-0171
34. Kumazawa K, Sawada T, Yanagisawa T, Shintani S (2012) Effect of single-dose amoxicillin on rat incisor odontogenesis: a morphological study. Clin Oral Investig 16:835–842. https://doi.org/10.1007/s00784-011-0581-4
35. DenBesten PK, Yan Y, Featherstone JD, Hilton JF, Smith CE, Li W (2002) Effects of fluoride on rat dental enamel matrix proteinases. Arch Oral Biol 47:763–770. https://doi.org/10.1016/s0003-9969(02)00117-6
36. Tye CE, Antone JV, Bartlett JD (2011) Fluoride does not inhibit enamel protease activity. J Dent Res 90:489–494. https://doi.org/10.1177/0022034510390043
37. Suzuki M, Shin M, Simmer JP, Bartlett JD (2014) Fluoride affects enamel protein content via TGF-β1-mediated KLK4 inhibition. J Dent Res 93(10):1022–1027. https://doi.org/10.1177/0022034514545629
38. Nanci A, Zalzal S, Lavoie P, Kunikata M, Chen W, Krebsbach PH, Yamada Y, Hammarström L, Simmer JP, Fincham AG, Snead ML, Smith CE (1998) Comparative immunochemical analyses of the developmental expression and distribution of ameloblastin and amelogenin in rat incisors. J Histochem Cytochem 46:911–934. https://doi.org/10.1177/002215549804600806

39. Dhamija S, Krebsbach PH (2001) Role of Cbfa1 in ameloblastin gene transcription. J Biol Chem 276:35159–35164. https://doi.org/10.1074/jbc.M010719200
40. Wald T, Osickova A, Sulc M, Benada O, Semeradtova A, Rezabkova L et al (2013) Intrinsically disordered enamel matrix protein ameloblastin forms ribbon-like supramolecular structures. J Biol Chem 288:22333–22345. https://doi.org/10.1074/jbc.M113.456012
41. Iwasaki K, Bajenova E, Somogyi-Ganss E, Miller M, Nguyen V, Nourkeyhani H, Gao Y, Wendel M, Ganss B (2005) Amelotin: a novel secreted, ameloblast-specific protein. J Dent Res 84:1127–1132. https://doi.org/10.1177/154405910508401207
42. Joseph BK, Harbrow DJ, Sugerman PB, Smid JR, Savage NW, Young WG (1999) Ameloblast apoptosis and IGF-1 receptor expression in the continuously erupting rat incisor model. Apoptosis 4:441–447. https://doi.org/10.1023/a:1009600409421
43. DenBesten PK, Crenshaw MA, Wilson MH (1985) Changes in the fluoride-induced modulation of maturation stage ameloblasts of rats. J Dent Res 64:1365–1370. https://doi.org/10.1177/00220345850640120701
44. Suga S, Aoki H, Yamashita Y, Tsuno M, Ogawa M (1987) Disturbed mineralization of rat incisor enamel induced by strontium and fluoride administration. Adv Dent Res 1:339–355. https://doi.org/10.1177/08959374870010022601
45. Richards A, Likimani S, Baelum V, Fejerskov O (1992) Fluoride concentrations in unerupted fluorotic human enamel. Caries Res 26:328–332. https://doi.org/10.1159/000261463

Figures

Figure 1

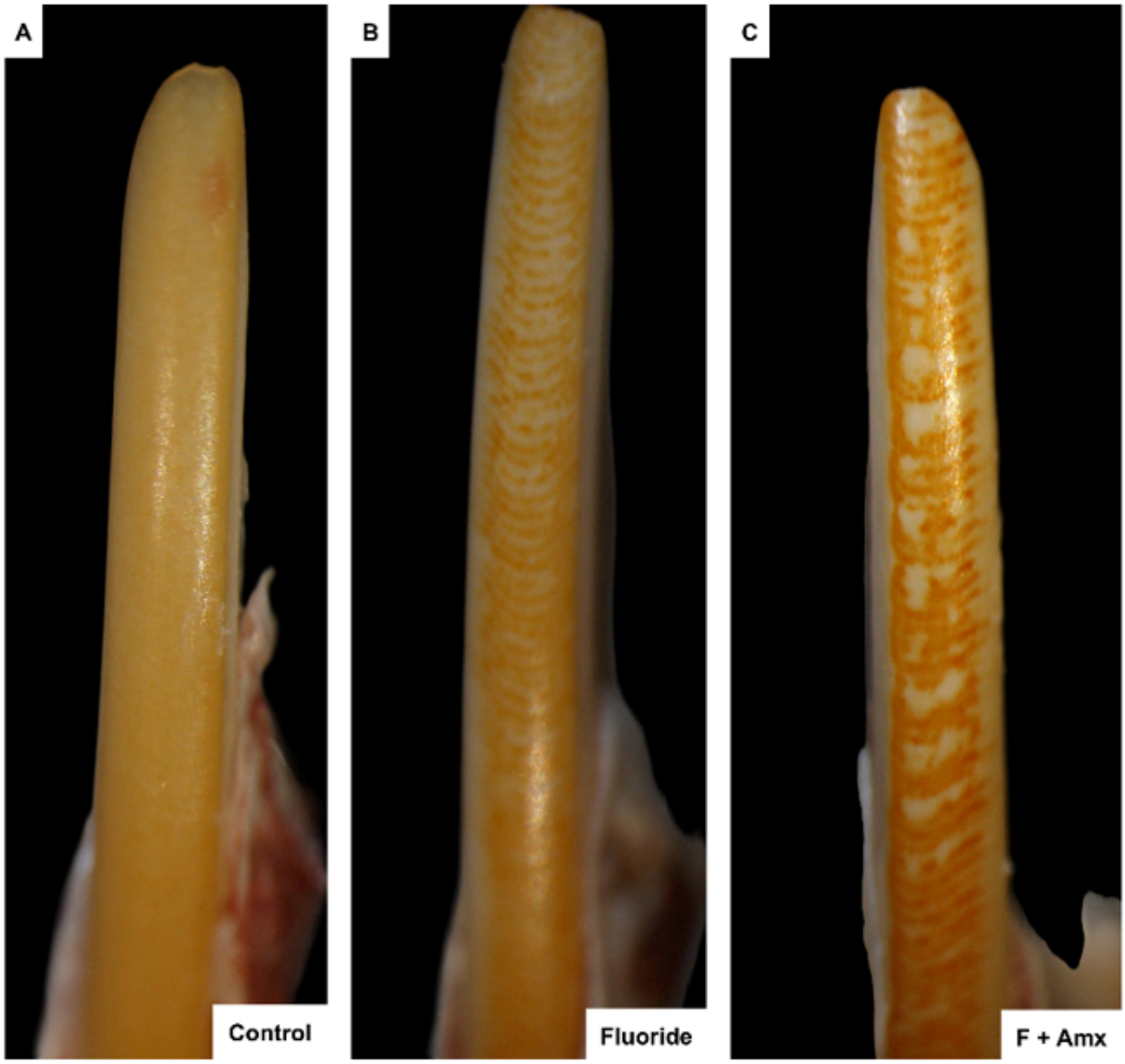

Figure 1

Photographs of the lower incisors. (A) Control group. (B) Fluoride group. (C) Fluoride plus amoxicillin group (F + Amx). Enamel striations are observed in the fluoride-treated group (B) and are more pronounced in the group treated concomitantly with amoxicillin (C). Original magnification: 10×.

Figure 2

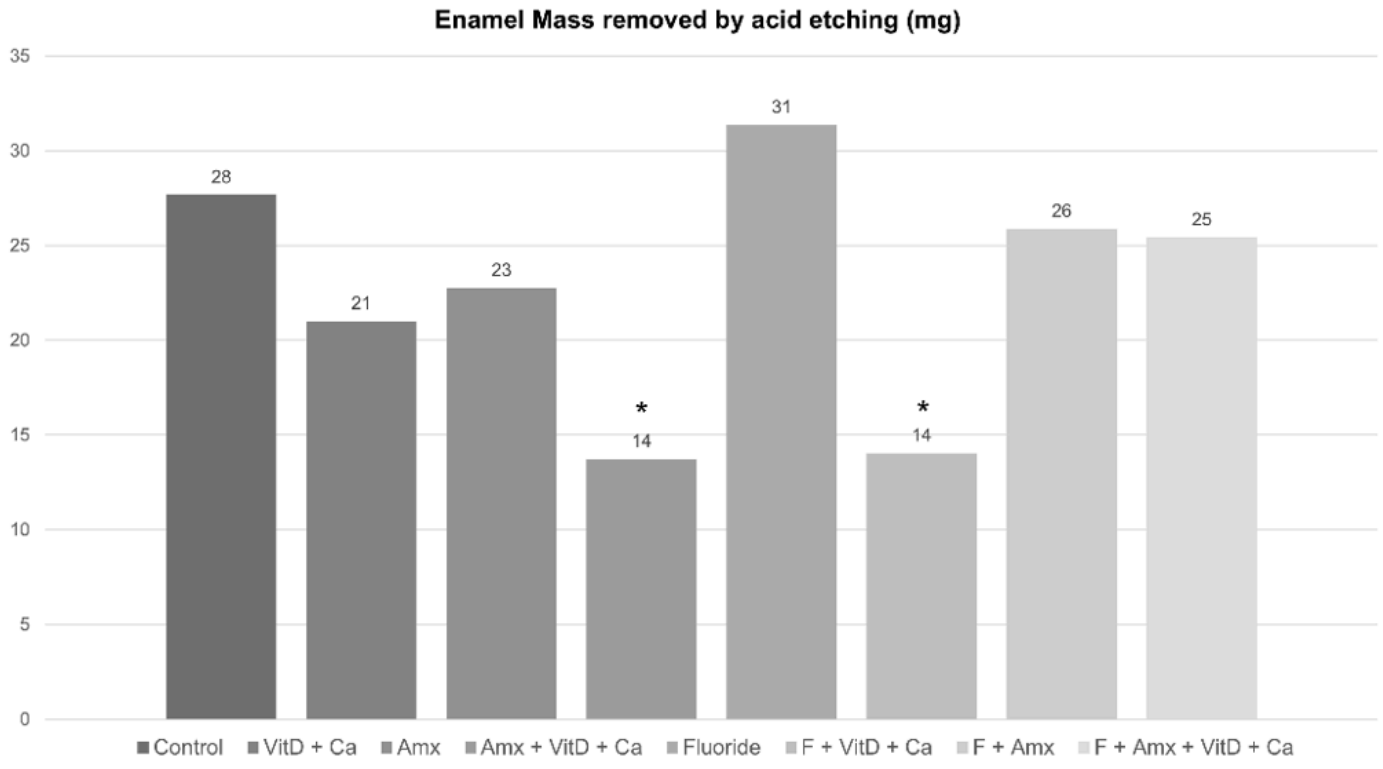

Figure 2

Enamel mass removed by superficial acid etching of the lower incisor. Dental enamel from the fluoride + vitamin D + calcium (F + VitD + Ca) and amoxicillin + vitamin D + calcium (Amx + VitD + Ca) groups showed higher resistance to acid dissolution. *p ≤ 0.05.

Figure 3

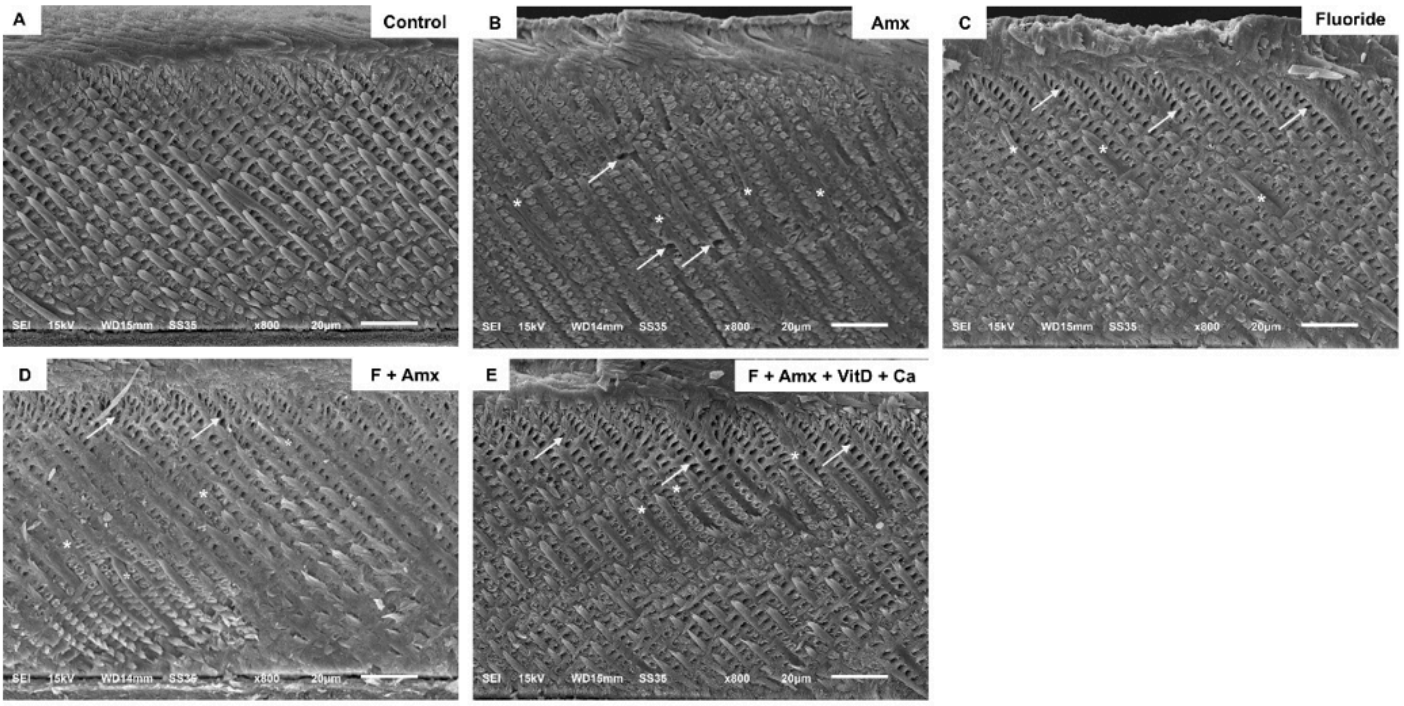

Figure 3

Scanning electron microscopy. The experimental groups exhibit thinner prismatic enamel compared with the control group (asterisks), whereas the interprismatic enamel shows an increased diameter (white arrows). Magnification: 800×.

Figure 4

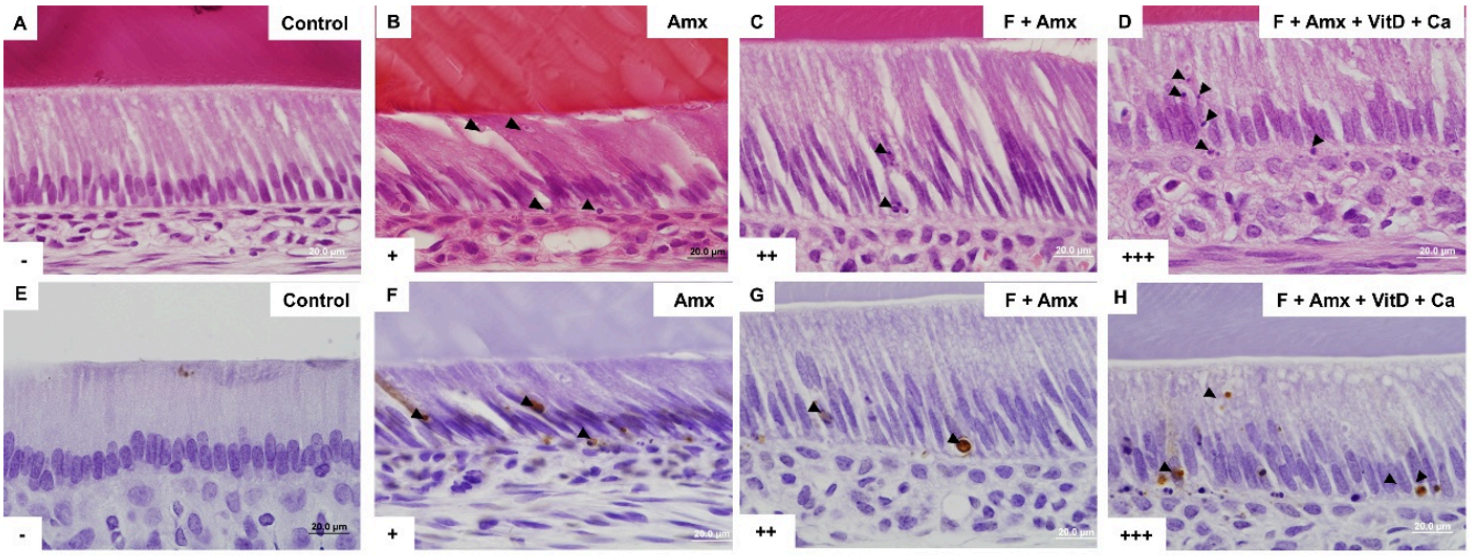

Figure 4

(A–C) **Hematoxylin and eosin staining.** (D–F) **TUNEL reaction.** In the H&E

staining, the amoxicillin, fluoride plus amoxicillin, and fluoride plus amoxicillin plus

vitamin D and calcium groups showed the presence of apoptotic bodies (A–C, arrowheads). Apoptosis was confirmed by positive TUNEL staining (D–F, arrowheads). Original magnification: 1000×. Qualitative assessment of apoptotic bodies in dental enamel. Scoring criteria: (–) absence of apoptotic bodies; (+) few apoptotic bodies; (++) moderate number of apoptotic bodies; (+++) large number of apoptotic bodies.

Figure 6

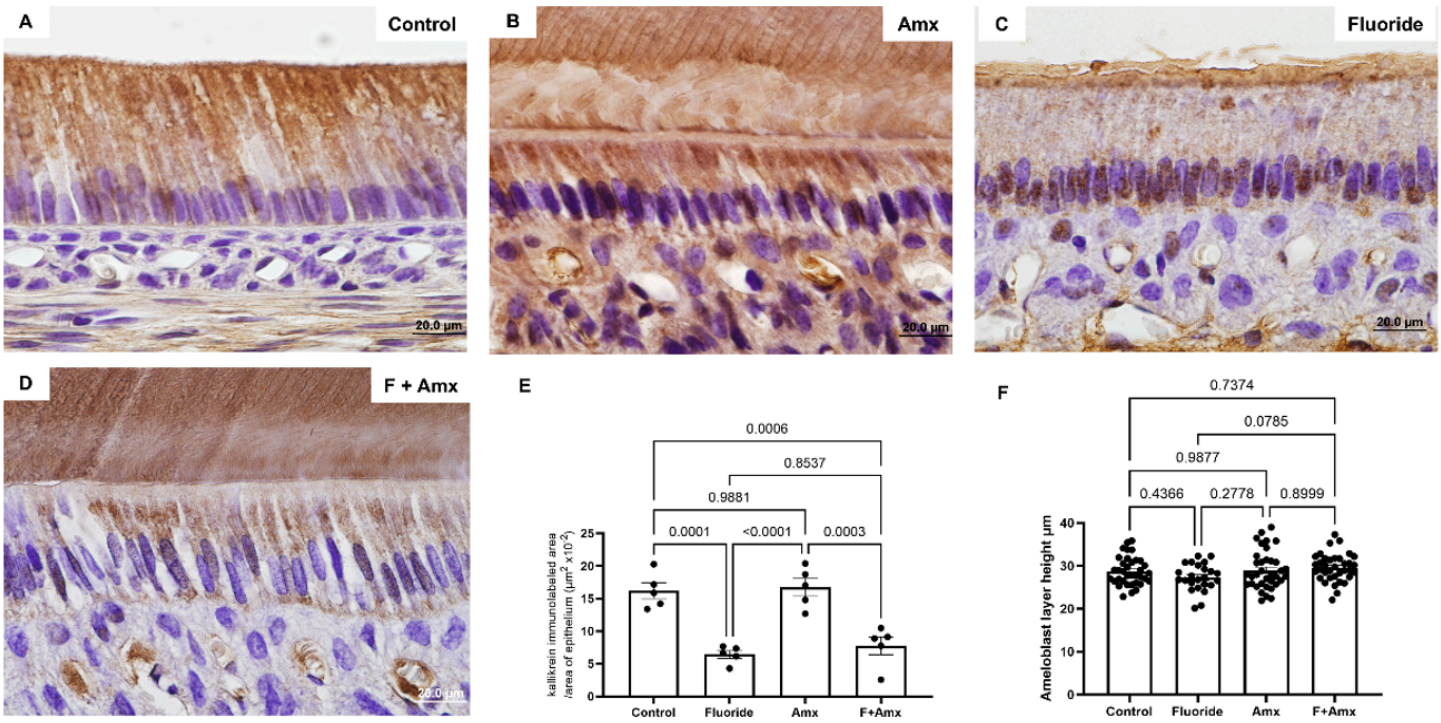

Figure 6

Immunohistochemistry for KLK4. The fluoride-treated groups (C-D) showed reduced KLK4 immunoreactivity compared with the control and amoxicillin groups (A-B). This difference was statistically significant (E) ($p < 0.01$). Measurement of ameloblast height (µm) in the region used for KLK4 immunolabeling showed no significant differences among groups (F), indicating that ameloblasts were in the same stage of amelogenesis (post-secretory stage). A-D: Original magnification: 1000×.

Supplementary Files

This is a list of supplementary files associated with this preprint. Click to download.

- supplementarytable.docx